Simulation of the Swelling of High-Volatile Bituminous Coal during Pyrolysis

ARTICLE *in* ENERGY & FUELS · NOVEMBER 2014

Impact Factor: 2.79 · DOI: 10.1021/ef5016846

4 AUTHORS, INCLUDING:

He Yang
Dalian University of Technology
5 PUBLICATIONS **14** CITATIONS
SEE PROFILE

Thomas H. Fletcher
Brigham Young University - Provo Main Campus
155 PUBLICATIONS **2,299** CITATIONS
SEE PROFILE

energy&fuels

Article

pubs.acs.org/EF

Simulation of the Swelling of High-Volatile Bituminous Coal during Pyrolysis

He Yang,[†,‡] Sufen Li,*[,†] Thomas H. Fletcher,[‡] and Ming Dong[†]

[†]School of Energy and Power Engineering, Dalian University of Technology, Dalian 116024, China

[‡]Chemical Engineering Department, Brigham Young University, Provo, Utah 84602, United States

ABSTRACT: In this paper, a model is established to predict the swelling ratio of high-volatile bituminous coal during pyrolysis, based on the assumption that the structure of bubble distribution in the particle at the beginning of the plastic stage is a central bubble surrounded by many surrounding bubbles. The initial number and size of the bubbles when the particles become plastic are calculated by the pressure in the particle. The chemical percolation devolatilization (CPD) model is used to describe pyrolysis. The pyrolysis of eight types of high-volatile bituminous coals is simulated, and the results are compared with experimental results to verify the model. The particle size during pyrolysis increases then decreases during pyrolysis. The model predicts experimentally observed trends in swelling ratio with heating rate; particle swelling during pyrolysis increases with heating rate, up to ~10^4 K/s, and then decreases with further increases in heating rate. Predictions of increasing then decreasing swelling with increases in ambient pressure also agree with trends that have been observed experimentally.

1. INTRODUCTION

During pyrolysis, the viscosity of the coal particle first increases and then decreases,[1,2] and when the viscosity of coal particle is smaller than a specified value, the particle becomes plastic.[3,4] Devolatilization is divided into three stages: the preplastic stage, the plastic stage, and the resolidified stage.

In the plastic stage, during the pyrolysis of high-volatile bituminous coal, particles become plastic and swell, depending on the heating rate and the external pressure.[2] This change in diameter during pyrolysis directly influences the porosity, inner surface area, and apparent density, which, in turn, affects the effective char reaction rate and formation of ash.[5−7] Therefore, the description of the swelling evolution during devolatilization is essential to a complete description of coal conversion for high-volatile bituminous coal.

The formation mechanism of char structure during pyrolysis has been researched widely in recent years.[8] During the plastic stage of the pyrolysis of high-volatile bituminous, the particle pore structure collapses, because of fluidic Metaplast. The volume of the pores is divided into many small parts to form bubbles and the volatile gases are trapped in the bubbles. The growth, coalescence, and rupture of the bubbles lead to the swelling and shrinking of the coal particle during pyrolysis. A dynamic variation of the particle size because of multiple ruptures during coal pyrolysis has been observed,[9,10] and, overall, the change of particle size is an increasing then decreasing trend. Studies at low heating rates in thermogravimetric analysis (TGA) devices and wire mesh reactors indicate that the final swelling ratio of coal particle increases as the heating rate increases;[11] however, studies with drop-tube furnaces and flat-flame burners show that the swelling ratios decrease at rapid heating rates.[12,13] Studies in elevated pressure reactors indicate that the coal swelling ratio also has the same increasing then decreasing trend with increasing ambient pressure.[6,14,15]

A few models have been developed by different investigators to describe the swelling of coal particles. A single bubble model was proposed by Solomon et al.[16] This model was employed by Sheng et al.[4] while considering gas diffusion in the porous shell of the particle to improve the model. The single bubble model can predict the final swelling ratio of coal particle; however, since the single bubble assumption is too simple, the model cannot explain the phenomenon that the number of bubbles in the particle changes with the heating condition[17] and cannot predict the decreasing trend of particle size during the late stage of pyrolysis at rapid heating rates. Oh et al.[3] proposed the multiple bubble model, based on the assumption that the rupture of bubbles at surface of the particle is the main way for volatile flow out of a particle. Yu et al. combined the multiple bubble model with the single bubble model to consider the single bubble stage during swelling with the multiple bubble initial condition.[18,19] The multiple bubble model predicts the increasing then decreasing trend of particle size during pyrolysis successfully. However, at a rapid heating rate (greater than 10^4 K/s), the multiple bubble model cannot predict the decrease in swelling with increasing heating rate. Also, the initial number of the bubbles in the particle in the multiple bubble model was set at a certain value by experience, which lacks a theoretical basis. An empirical swelling correlation as a function of coal rank, heating rate, and ambient pressure was proposed by Fletcher et al.[13,15] The correlation correctly describes experimentally observed trends with the heating rate and ambient pressure. However, the correlation was obtained from fitting data from the literature, not considering the pressure changes in the particle during pyrolysis, so it cannot describe the particle swelling with a mechanism based on mechanical properties.

Received: July 26, 2014
Revised: October 20, 2014
Published: October 20, 2014

dx.doi.org/10.1021/ef5016846 | *Energy Fuels* 2014, 28, 7216−7226

Moreover, none of the existing models considered the influence of the pressure inside the particle on swelling at the end of the preplastic stage before plastic deformation. In most studies on pyrolysis, the pressure inside the solid particle is regarded as being equal to the ambient pressure. At rapid heating rates, however, large amounts of gases are generated from pyrolysis within a short time. Some gases are restrained by the solid phase, amassed in the pores.[20,21] Yang et al. simulated the evolution of the internal pressure of a lignite particle during pyrolysis and found the pressure in the pores to be 2.6 times larger than the ambient pressure at the heating rate of 1×10^4 K/s and an ambient pressure of 0.1 MPa.[22] The internal pressure at the end of the preplastic stage could influence the final swelling ratio by affecting the initial distribution of pressure in the particle and the formation of bubbles at the beginning of the plastic stage.

In this paper, a model is established to predict the swelling ratio of high-volatile bituminous coal during pyrolysis. The multiple bubble model is combined with a single bubble model. The influence of the pressure in the particle at the end of the preplastic stage on the initial number and size of bubbles in the plastic stage is considered in the model. The initial structure of bubble distribution in the particle at the beginning of the plastic stage is assumed as a central bubble surrounded by many surrounding bubbles, and the coalescence between the central bubble and the surrounding bubbles is considered in the model. The swelling of a set of high-volatile bituminous coals during pyrolysis is simulated. The simulation results are compared with experimental results to evaluate the model, and the influences of heating conditions on particle swelling are analyzed.

2. MODELING

To simulate the swelling process of the coal particle during pyrolysis, the change of the number and the size of bubbles must be calculated. The process of bubble formation, coalescence, and rupture must be modeled.

2.1. Assumptions. (1) The coal particle is spherical and isotropic, so there is no pressure or velocity gradient in circumferential direction;

(2) In the preplastic stage, the coal particle is a porous medium with continuous cylindrical pores with no fragmentation or thermoplastic deformation during pyrolysis;[22]

(3) During the process of macropores converting to bubbles, the total volume of macropores remains constant;

(4) In the plastic stage, the structure of bubble distribution in the particle is one central bubble surrounded by many surrounding bubbles. This assumption is based the following deduction:

- Bubbles originate from macropores in the coal at the onset of the plastic stage.[3] At the beginning of the plastic stage, the force balance in each cross section of a pore consists of the surface tension of the Metaplast and the pressure difference between the inside and the outside of the pore. When the surface tension of the Metaplast is larger than the pressure difference between the inside and the outside of the pore, the force can decrease the pore diameter until the pore closes, and bubbles will be formed. In the preplastic stage, some gases are restrained by the solid structure and are amassed in the pores. The pressure increases from the boundary to the core of the particle. At rapid heating rates, the pressure in the core of the particle is much higher than the ambient pressure.[22] At the beginning of plastic stage, if $P_{pore} - P_\infty - 2\sigma/r_{pore} > 0$ in the core of the particle, the pore diameters increase, which will decrease the value of surface tension and make the value of $P_{pore} - P_\infty - 2\sigma/r_{pore}$ increase, and the pores cannot be closed. However, in the outer edge of the particle, the pressure may be lower ($P_{pore} - P_\infty - 2\sigma/r_{pore} < 0$) and the pores may be closed. The pores are divided into many small parts to form bubbles. Under the effect of surface tension, the closed pore walls will push the gases in the core to gather in the center of the particle, and the gases in the core also push the Metaplast from the core to the outside. Hence, the central bubble is formed.
- In the actual pyrolysis, the initial sizes of the bubbles in the particle at the beginning of plastic stage are different, and the bubbles can coalesce with each other. The assumption of a central bubble with surrounding bubbles is easy for calculating the coalescence between the central bubble and the surrounding bubbles. Therefore, the coalescence between bubbles can be considered, although the coalescence between the surrounding bubbles is neglected, based on the idea that the coalesced surrounding bubbles will also coalesce with the central bubble and become part of the central bubble, or finally rupture on the surface of the particle. This method is more reasonable than the multibubble model of Yu et al.,[19] which is based on the assumption that the size and spatial distribution of bubbles were uniform in a molten coal particle during the plastic stage and the coalescence of bubbles was totally neglected.

(5) In the plastic stage, the pressure gradient that existed in the preplastic stage is disturbed by the molten Metaplast. Therefore, there is no pressure gradient in the particle in the radial direction, and the number density of surrounding bubbles does not change with particle radius.

2.2. CPD. In this paper, the pyrolysis reaction is described by the chemical percolation devolatilization (CPD) model.[23−25] The CPD model includes (a) a description of the chemical structure of the parent coal, (b) a kinetic scheme for breaking labile bonds and side chains, (c) percolation statistics based on a Bethe lattice for freeing molecules from the coal particle, (d) a vapor−liquid equilibrium treatment of Metaplast versus tar, and (e) a cross-linking mechanism for reattaching Metaplast to the solid char. The average internal pressure in the particle is used as the reaction pressure in the CPD model instead of the external pressure. In the preplastic stage, the average internal pressure in the particle is obtained by the computational fluid dynamics (CFD) method.[22] In the plastic stage, the average internal pressure at each time step is estimated by an area-weighted method, as shown in eq 1,

$$\overline{P} = \frac{\sum r_b^2 P_b + P_\infty R_p^2}{\sum r_b^2 + R_p^2} \quad (1)$$

where r_b is the radius of each bubble, P_b the pressure in the bubble, P_∞ the ambient pressure, and R_p the radius of the particle.

2.3. Viscosity of the Coal Particle. The temperature-dependent viscosity of the coal particle is expressed as shown in eq 2,[3,4,19]

dx.doi.org/10.1021/ef5016846 | Energy Fuels 2014, 28, 7216−7226

$$\mu = \frac{1 \times 10^{-11} \exp(45000/RT)}{(1 - \phi_m)^{-1/3} - 1.0} \quad (2)$$

where ϕ_m is the Metaplast content in the coal melt and the temperature (T) is set to 723 K when $T > 723$ K.

The critical viscosity value (μ_c) in this work is set to 1×10^4 Pa s, which is the same as that determined by Yu et al.[19]

2.4. Preplastic Stage. The evolution of pressure in the particle is simulated using a CFD method for gas motion in porous media, which has been applied successfully on the simulation of the evolution of internal pressure in a nonswelling coal.[22]

In spherical coordinates, the gas continuity equation in porous media is described as

$$\theta\frac{\partial \rho}{\partial t} + \frac{1}{r^2}\frac{\partial(\rho\rho^2 U)}{\partial r} - \frac{\mathrm{d}m}{\mathrm{d}t} = 0 \quad (3)$$

where U is the average velocity through the sphere of radius r, m the yield of volatiles at time t, and θ the porosity.

The differential equation of gas motion in porous media is shown in eq 4:

$$\theta^{-1}\frac{\partial \rho U}{\partial t} + \theta^{-2}U\frac{\partial \rho U}{\partial r} = -\left(\frac{\mu}{K}\right)U - \frac{1}{r^2}\frac{\partial(Pr^2)}{\partial r} \quad (4)$$

where P is the pressure, μ is the viscosity of the volatile gas, and K is expressed as

$$K = K_0\left(1 + \frac{29}{3\mathrm{e}^{-2r_k/\bar{\lambda}}}\right) \quad (5)$$

where K_0 is the absolute permeability $(K_0 = \theta/(8{r_k}^2))$; r_k is the pore radius $(r_k = 2r_f\theta/\rho_c s_c$, where s_c is the N_2 BET surface area (and, because the N_2 BET surface area of bituminous changes little during pyrolysis,[26] s_c is set to 5 m^2/g)); r_f is the roughness factor;[27] and $\bar{\lambda}$ is the average free path of molecule, which is described as

$$\bar{\lambda} = \frac{kT}{\sqrt{2}\pi {d_{\mathrm{mol}}}^2 p} \quad (6)$$

where k is the Boltzmann constant, and d_{mol} is the average molecular diameter of gases.

A staggered-grid finite volume mesh is adopted. The particle is divided into 351 pressure grids and 350 velocity grids in the radial direction. Pressure and velocity grids are staggered. The grid spacing is set to $R_p/350$, and the first point of the pressure grid is the center of the sphere.

The average diameter of pores in the coal particle, the pressure and the pressure distribution at the end of the preplastic stage are used as the initial conditions for the plastic stage.

2.5. Resolidified Stage. After the plastic stage, the change of particle size is small, so the diameter is assumed to be constant during this stage.

2.6. Formation of Bubbles. At the beginning of the plastic stage, the pore system in the particle collapses with the flow of Metaplast, and the gases are divided into many small parts to form bubbles.

Bubbles originate from macropores in the coal at the onset of the plastic stage.[3] The initial radius of the bubbles $({r_b}^0)$ should be between the radius of a macropore (r_{pore}) and the radius of the bubble when the force in the bubble is balanced (r_b^{fb}):

$$r_{\mathrm{pore}} \le r_b^0 \le r_b^{\mathrm{fb}} \quad (7)$$

The radius of the bubble when the force in the bubble is balanced is calculated as follows:

$$r_b^{\mathrm{fb}} = \frac{2\sigma}{P_b^0 - P_\infty} \quad (8)$$

where P_b^0 is the initial pressure in the bubble, which is set to be equal to the final pressure in the pore at the end of the preplastic stage; P_∞ is the ambient pressure, and σ is the surface tension of coal melt, which is set to 0.03 N/m (the same value used by other researchers).[3,4,28]

2.6.1. Central Bubble. The initial volume of the central bubble is equal to the total volume of macropores in the area where $r_b^{\mathrm{fb}} < r_{\mathrm{pore}}$, so the initial radius of the central bubble becomes

$$r_{b1}^0 = \left(\frac{{r_e}^3/{r_p}^3 m_p \hat{V}_{\mathrm{pore}}}{4/3\pi}\right)^{1/3} \quad (9)$$

where r_e is the distance between the core of the particle and the point where $r_b^{\mathrm{fb}} = r_{\mathrm{pore}}$. If the internal pressure is not high enough, and at the core in the particle $r_b^{\mathrm{fb}} \ge r_{\mathrm{pore}}$, r_e is set to $R_p/700$ in the computation, which is the radius of the first velocity grid in the particle. In addition, m_p is the initial mass of the coal particle, $\hat{V}_{\mathrm{pore}}$ is the volume of macropores per unit mass of coal at the beginning of the plastic stage.

$$\hat{V}_{\mathrm{pore}} = \hat{V}_{\mathrm{pore}}^0 + f_v(1 - \theta_0)\frac{\hat{V}_{\mathrm{pore}}^0}{\theta_0 V_p^0} \quad (10)$$

where $\hat{V}_{\mathrm{pore}}^0$ is the initial volume of macropores per unit mass of coal (it is set to 2.4×10^4 m^3/kg, which is the average volume of macropores of bituminous coal),[29] θ_0 the initial porosity of the coal particle, V_p^0 the initial volume of the coal particle, and f_v the fraction of volatile yield.

2.6.2. Bubbles around Central Bubble. 2.6.2.1. Initial Radius of Surrounding Bubbles. The initial radius of the surrounding bubbles is between the radius of the pore at the beginning of the plastic stage and the radius of the bubbles when the force in the bubble is balanced. The radius of the bubbles is different at different places in the particle because of the pressure gradient in the particles. The initial radius of the bubble under the pressure P_i is described as eq 11:

$$r_{b0}^i = f_r\left(\frac{2\sigma}{P_i - P_\infty}\right) + (1 - f_r)r_{\mathrm{pore}} \quad (11)$$

where f_r is an adjustable parameter $(0 \le f_r \le 1)$; in this paper, it is set to a value of $f_r = 0.4$.

2.6.2.2. Initial Number of Surrounding Bubbles. The macropores surrounded by continuous Metaplast can convert to bubbles and the initial number of bubbles at pressure P_i can be described by eq 12:

$$n_{b0}^i = \frac{\hat{V}_{\mathrm{pore}} m_p^0 f_{\mathrm{volume}}^i}{4/3\pi {r_{b0}^i}^3}\phi_m\theta_{\mathrm{ma}}f_{\mathrm{VP}} \quad (12)$$

where f_{volume}^i is the volume fraction at pressure P_i and θ_{ma} is the porosity of the macropores.

During pyrolysis, the solid phase and the Metaplast are scattered throughout the particle. If the distance between two groups of Metaplast is large enough to make them unable to

dx.doi.org/10.1021/ef5016846 | Energy Fuels 2014, 28, 7216−7226

Table 1. Coal Parameters

coal	C (%, daf)	H (%, daf)	N (%, daf)	O (%, daf)	volatiles (%, daf)	ash (%, dry)
Illinois No. 6	76.68	5.54	1.45	12.73	44.27	8.46
Pittsburgh No. 8	82.19	5.42	1.58	8.58	38.8	6.57
Blue No. 1	75.6	5.26	1.32	0.49	17.33	3.48
Hiawatha	79.69	5.27	1.22	13.38	37.24	7.17
Eastern Bituminous	79.08	5.84	1.49	12.59	47.87	7.36
Australian Bituminous	83.7	5.45	1.81	8.6	30.4	15.1
Adaville No. 1	70.64	5.32	1.03	21.98	44.57	3.33
Kentucky No. 9	77.01	5.61	1.69	11.69	46.27	8.07

connect with each other, they cannot trap the pore volume to form a bubble. In a larger particle, the Metaplast can be more easily divided into separate groups; therefore, there should be a factor related to the volume of the particle. Therefore, an influence factor for the particle volume (f_{VP}) is used to correct the number of bubbles in eq 12, where f_{VP} is calculated as follows:

$$f_{VP} = 6.0 \times \left(\frac{26 \times 10^{-6}}{r_{p0}}\right)^3 \tag{13}$$

The value of f_r and the form of eq 13 are obtained from fitting experimental data.

2.7. The Growth Rate of Bubbles. The growth rate of bubbles is described by a force balance,[3,4,19] as shown in eq 14:

$$\frac{dr_b}{dt} = \frac{r_b}{4\mu}\left(P_b - P_\infty - \frac{2\sigma}{r_b}\right) \tag{14}$$

where r_b is the radius of the bubble and the pressure in the bubble is described in eq 15.

$$P_b = \frac{n_m^b R T_p}{V_b} \tag{15}$$

where V_b is the volume of the bubble, T_p is the temperature of the particle, R is the gas constant. n_m^b is the number of moles of volatile matter inside each bubble, as described in eq 16:

$$n_m^b = \int \frac{R_t}{M_v}\frac{r_b^2}{\sum r_b^2 + R_p} dt \tag{16}$$

where R_t is the rate of pyrolysis, based on the CPD model, and M_v is average molecular weight of gases.

2.8. Change in Bubble Number. Changes in the number of bubbles can happen by bubble rupture or bubble coalescence. Treatments of these effects are described below.

2.8.1. Rupture Rate of Surrounding Bubbles. Surrounding bubbles rupture when they contact the particle surface, thereby releasing their inventory of volatiles outside the particle. The corresponding rate of bubble collisions with the particle surface is

$$\text{rate of bubble collisions (particle surface)} = 4\pi(R_p - r_b)^2 r_b n_b^v \tag{17}$$

where n_b^v is the number of bubbles per unit volume of original coal.

The escape rate of the bubbles is as shown in eq 18, which is the same equation used by Oh et al.[3] and Yu et al.:[15]

$$\left(\frac{dn_b}{dt}\right)_r = -\frac{4\pi(R_p - r_b)^2}{\frac{4\pi}{3}R_{p0}^3}\frac{dr_b}{dt}n_b \tag{18}$$

where R_{p0} is the initial radius of the particle.

2.8.2. Coalescence Rate of Surrounding Bubbles with the Center Bubble. Surrounding bubbles coalesce with the center bubble when they contact the center bubble surface. The corresponding rate of bubble collisions with the center bubble surface is

$$\text{rate of bubble collisions (center bubble surface)} = 4\pi(r_c + r_b)^2 r_b n_b^v \tag{19}$$

where r_c is the radius of the center bubble.

The coalescence is led not only by the expansion of the surrounding bubble, but also by the expansion of the central bubble. Therefore, the coalescence rate is estimated as shown in eq 20. The volume of the new central bubble after coalescence is equal to the sum of the volume of the central bubble before coalescence and the surrounding bubbles coalescing into the central bubble.

$$\left(\frac{dn_b}{dt}\right)_c = -\frac{4\pi(r_c + r_b)^2}{\frac{4\pi}{3}R_{p0}^3}\frac{d(r_b + r_c)}{dt}n_b \tag{20}$$

2.9. Single Bubble Stage. As the number of bubbles decreases to 1 and a cenospheric structure is formed, the single bubble model is applied.[4] The growth rate of the bubble is described by eq 21.

$$\frac{dr_b}{dt} = \frac{r_b}{4\mu}\left(p_b - p_\infty - \frac{\sigma}{r_b} - \frac{\sigma}{R_p}\right) \tag{21}$$

As the internal pressure increases to a specified value, the bubble ruptures. At rupture, the volatiles contained in the bubble are released rapidly. The shell is assumed to close and contract under the surface tension to form a new bubble that retains volatiles at the pressure of the environment.[4] Under the surface tension, the bubble shrinks, and then with the generation of volatiles, the pressure in the bubble increases and the bubble swells again. The criteria for bubble rupture are defined using wall strength[4] as shown in eq 22. The critical wall stress (S_w) is set to $[P_\infty/(1.02325 \times 10^5)]^{2/3} \times 1.02325 \times 10^5$ Pa, which is the same as that reported by Yu.[19]

$$\frac{1.5 r_b^3 (P_b - P_\infty)}{R_p^3 - r_b^3} - P_\infty > S_w \tag{22}$$

2.10. Calculation Conditions. Pyrolysis of a 60-μm Illinois No. 6 bituminous coal particle is simulated. The heating conditions are the same as the coal pyrolysis experiment of

dx.doi.org/10.1021/ef5016846 | Energy Fuels 2014, 28, 7216−7226

Serio et al.[30] The results of simulation are compared with the results of experiment to verify the accuracy of the model.

The swelling ratios of eight types of high-volatile bituminous coals on the heating conditions in the literature (Illinois No. 6,[11,14,15,26] Pittsburgh No. 8,[6,12,15,26] Blue No. 1,[13,26] Hiawatha Bituminous,[13] Eastern Bituminous,[13] Australian Bituminous,[19] Adaville No. 1,[15] and Kentucky No. 9[15]) during pyrolysis are calculated to verify the accuracy of the model. The coal parameters are shown in Table 1. The heating rates range from 1×10^3 K/s to 2.24×10^5 K/s, ambient pressure ranges from 0.84 atm to 15 atm, and particle diameters range from 58 μm to 275 μm.

In addition, the pyrolysis of the 60-μm coal particles of Illinois No. 6 bituminous coal and Pittsburgh No. 8 bituminous coal at various heating rates and various heating ambient pressure were simulated to analyze the effects of heating conditions on swelling.

3. RESULTS AND DISCUSSION

3.1. Validation of the Model. The yields of volatiles in the simulation are compared with the Serio experiment[30] to verify the accuracy of the model. The simulation results agree well with the experimental results, as shown in Figure 1.

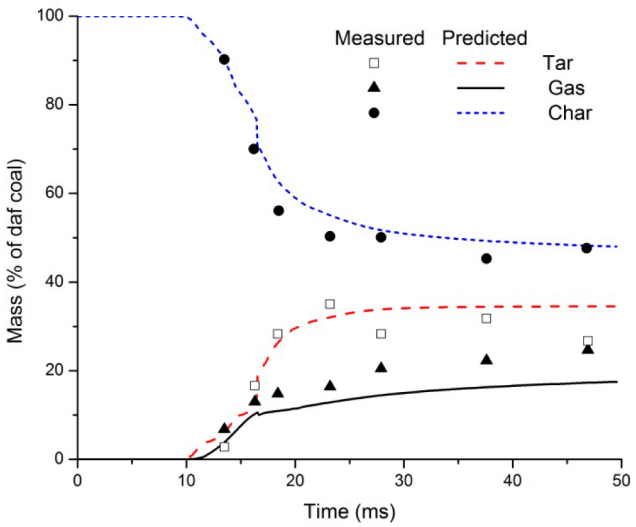

Figure 1. Comparison of the predicted yields with data from the Serio experiment.[30]

The final swelling ratios of eight high-volatile bituminous coals obtained by the model developed in this paper are compared to experimental data. Note that these experiments were performed using various heating conditions. Most of the simulation results agree well with the experimental results, as shown in Figure 2.

The change in particle size of Illinois No. 6 bituminous coals during pyrolysis, as predicted by the model, is compared to the data from the experiment by Fletcher and Hardesty,[26] as shown in Figure 3. The heating rate is 1.6×10^4 K/s, and the particle diameter is 115 μm. The trend in the change of swelling ratio predicted by the model agrees well with most of the experimental data points.

3.2. Changes in the Swelling Ratio of Coal. When the particle becomes plastic, the bubbles are generated. The volatile gases are accumulated in the bubbles, which make the pressure in the particle increase rapidly. The bubbles expand from the

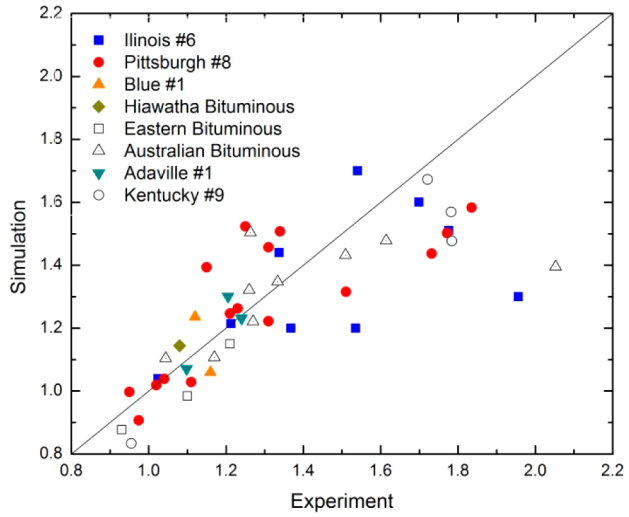

Figure 2. Comparison of the predicted final swelling ratio of coal particle to experimental data.

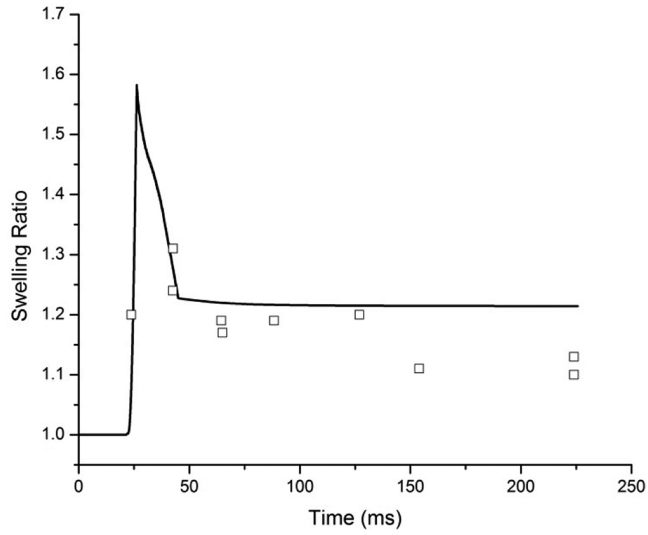

Figure 3. Comparison of the predicted change of coal swelling ratio to data from the Fletcher experiment[26] (Illinois No. 6 bituminous coal).

effect of pressure, and as the expansion reaches a certain value, when the expansion rate of the bubbles is larger than the volatile generation rate, the pressure decreases. However, the pressure in the bubble will be still larger than outside of the particle for some time, which makes the particle continue to swell. During the expansion, some surrounding bubbles escape out of the particle, some coalesce with the central bubble, and the amount of bubbles decreases gradually to 1. When the cenosphere structure is formed and the internal pressure is greater than the strength of the coal shell, the bubble ruptures. After rupture, the pressure rapidly decreases to ambient pressure. Under the effect of surface tension, the bubble will close again and shrink. However, the cenosphere structure is not stable. The radius of the central bubble is large, so the effect of surface tension is limited, and with the generation of volatiles, the central bubble is easy to rupture again. The particle size decreases rapidly because of the frequent shrinkages after the central bubble ruptures.

The evolution of average internal pressure and the swelling ratio for the Illinois No. 6 bituminous coal particle in the

dx.doi.org/10.1021/ef5016846 | Energy Fuels 2014, 28, 7216−7226

Fletcher experiment are shown in Figure 4, and the volatiles yield are shown in Figure 5. (Note that, because of the large

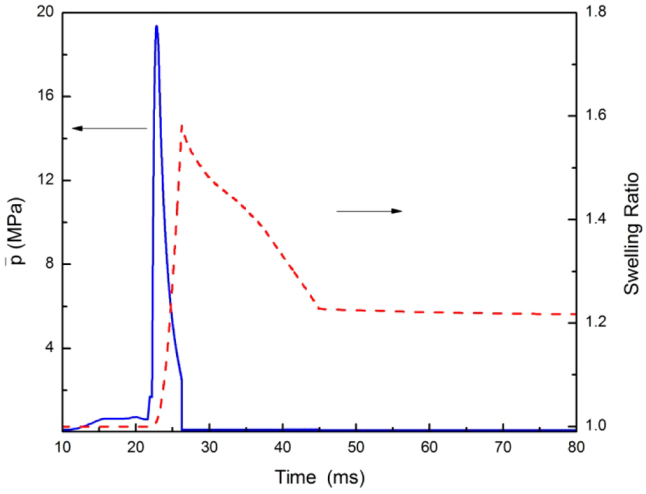

Figure 4. Predicted changes in average internal pressure and swelling ratio for Illinois No. 6 bituminous coal particles in the Fletcher experiment.[26]

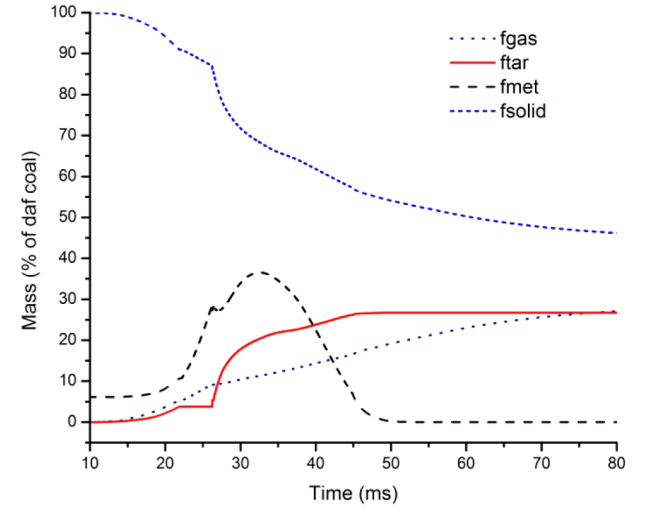

Figure 5. Predicted volatiles yield for Illinois No. 6 bituminous coal particles in the Fletcher experiment.[26]

internal pressure at plastic stage, there is a short duration, when the generation rate of tar is very small.) The change in the amount of bubbles, the central bubble size, and the particle size are shown in Figure 6.

At the beginning of the plastic stage, there are more than 3300 bubbles and the expansion of the surrounding bubbles contributes the most to the total expansion of particle. However, with the escape of surrounding bubbles outside the particle and their coalescence with the central bubble, the central bubble comprises the main part of the particle volume in the late plastic stage. The existence of one central bubble structure in the late plastic stage agrees with the char structure of only one or two big bubbles observed by Fletcher et al.,[26] and the existence of a multiple bubble stage can also explain the char structure of multiple bubbles observed by Griffin et al.[17]

3.3. Influence of Heating Rate. The pyrolysis of the 60-μm coal particles of Illinois No. 6 bituminous coal and

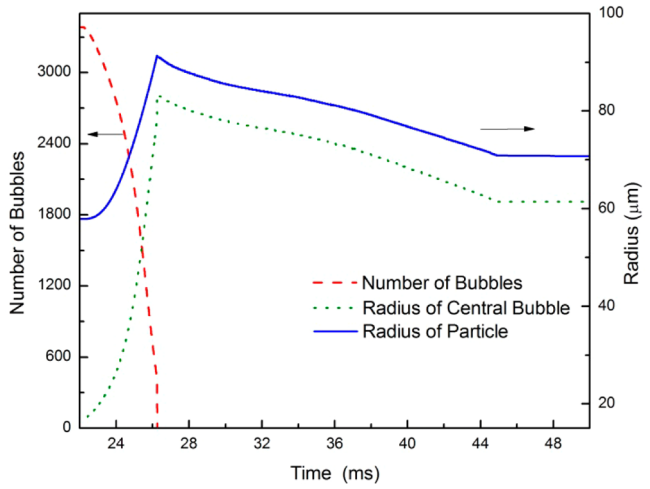

Figure 6. Predicted changes in the amount of bubbles, central bubble size, and particle size for Illinois No. 6 bituminous coal particles in the Fletcher experiment.[26]

Pittsburgh No. 8 bituminous coal at various heating rates and ambient pressure of 0.1 MPa are simulated. The final swelling increases at first and then decreases as the heating rate increases, as shown in Figure 7. This trend has been observed

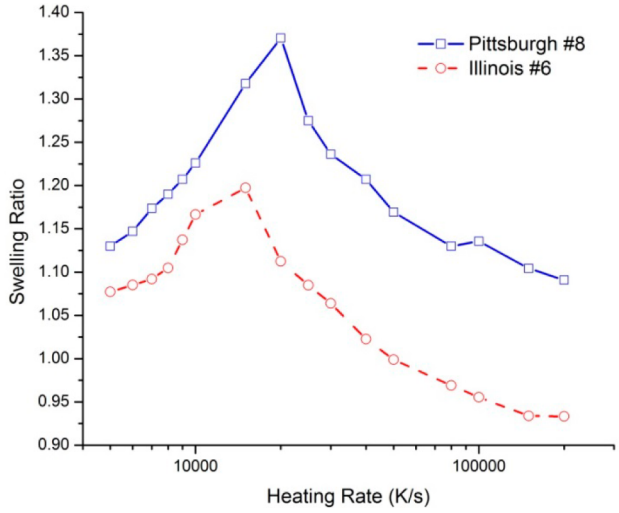

Figure 7. Final swelling ratio at various heating rates and an ambient pressure of 0.1 MPa for a particle 60 μm in diameter.

in similar experiments at heating rates from 1 K/s to 10^5 K/s. The swelling increases as the heating rates increase at heating rates below 10^4 K/s and then decreases rapidly at heating rates from 10^4 K/s to nearly 10^5 K/s.[13] However, this model can only calculate the particle swelling ratio at heating rates larger than 1×10^3 K/s when a single central bubble is assumed. Although swelling is thought to increase at heating rates from 10^3 to 10^4 K/s,[12,13] data for small particles are not available at heating rates between 1×10^3 K/s to 10^4 K/s. The trend predicted by the model at heating rates larger than 10^4 K/s is compared with data in Figure 8. Note that the data point at 10^3 K/s in Figure 8 for the Illinois coal was for a particle 275 μm in diameter; the corresponding prediction shown was also made for a particle 275 μm in diameter.

The increasing then decreasing trend of swelling ratio with increasing heating rates is explained in the following two points:

dx.doi.org/10.1021/ef5016846 | Energy Fuels 2014, 28, 7216−7226

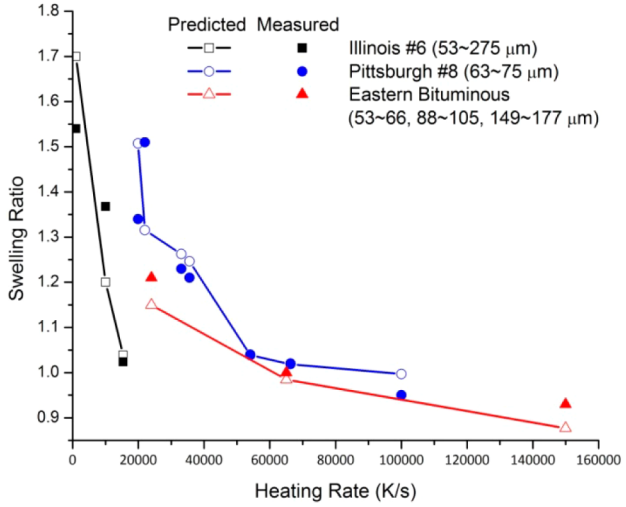

Figure 8. Comparison of the predicted and measured trends of final swelling ratio of coal particle with increasing heating rate at an ambient pressure of 0.1 MPa.[6,12,14,15] (The particle diameter was changed at each point to correspond to the measurments.)

(1) The internal pressure and its duration change as the heating rate increases. The internal pressure is larger at higher heating rates, as shown in Figure 9. A larger internal pressure

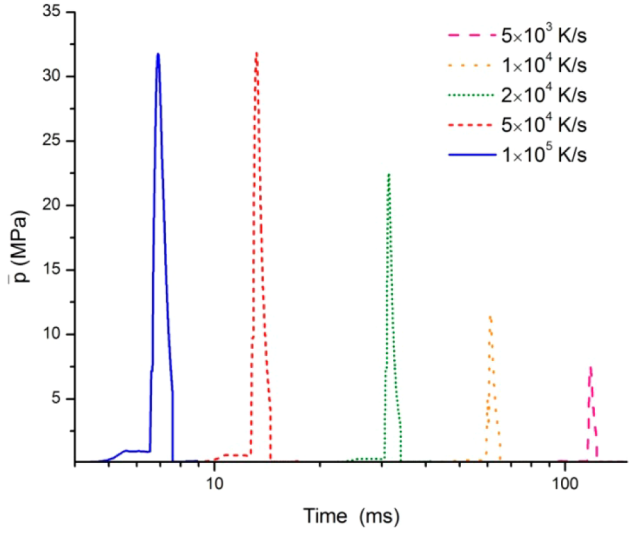

Figure 9. Transient internal pressure profiles at various heating rates and an ambient pressure of 0.1 MPa (Illinois No. 6 bituminous coals).

can provide a larger driving force for bubble expansion. However, increasing the pressure difference raises the rupture frequency and, hence, decreases particle swelling. In addition, at higher heating rates, the duration of the internal pressure peak is shorter. At a heating rate of 5×10^3 K/s, the duration of an average internal pressure greater than 2.5 MPa is ~5.5 ms, and at a heating rate of 1×10^5 K/s, it is only 0.3 ms. The decreased plastic deformation time reduces the swelling.

(2) The initial number of surrounding bubbles and their rupture rate at the particle surface change with an increase in heating rate. The initial pressure of the plastic stage increases with increasing heating rate, as shown in Figure 10. At higher pressures, the initial diameter of the bubble is small, and the number of bubbles is larger. Therefore, as heating rates increase

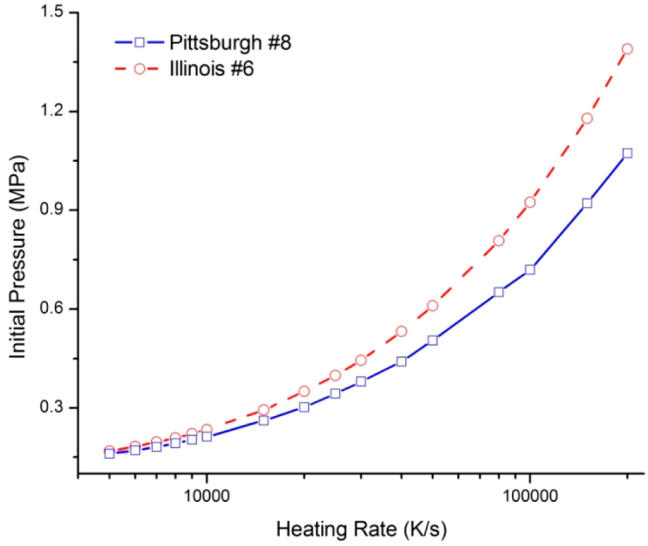

Figure 10. Initial pressure in the plastic stage at various heating rates and an ambient pressure of 0.1 MPa.

from 5×10^3 to 1×10^4 K/s, the initial number of bubbles increases from 1000 to more than 5000. However, at a higher internal pressure, when r_b^{fb} is smaller than r_{pore} at the core of the particle, the initial size of the central bubble increases with the increasing heating rate. The enlargement of the central bubble can decrease the initial number of bubbles. The initial number of bubbles and the initial central bubble radius in the plastic stage at various heating rates are as shown in Figure 11. More

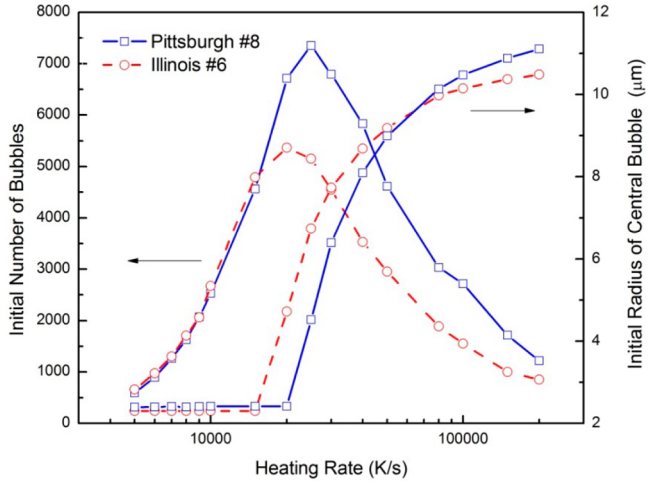

Figure 11. Initial number of bubbles and initial radius of the central bubble in the plastic stage at various heating rates and an ambient pressure of 0.1 MPa.

bubbles are better for particle expansion, so the swelling ratio and initial number of bubbles exhibit the same increasing and then exhibit a decreasing trend with increasing heating rate. Both of the knee points are at the heating rate where the initial size of the central bubble begins to increase. In addition, a larger central bubble makes the shell of the coal particle thinner, and this is better for bubbles flowing out of the particle. Therefore, at higher heating rates, the swelling ratio is smaller than at lower heating rates, even with the same initial number of bubbles.

dx.doi.org/10.1021/ef5016846 | Energy Fuels 2014, 28, 7216−7226

The influences of the internal pressure, the central bubble rupture frequency, the duration of internal pressure, and the initial bubble number in plastic stage are complicated. To determine the dominant factor for the increasing then decreasing trend of swelling ratio with increasing heating rates, four sets of computations for different computing conditions were performed, as outlined in Table 2.

Table 2. Conditions for Sensitivity Analysis of Swelling Ratio to S_w and n_{b0}^i

condition	critical wall stress, S_w	initial number of bubbles, n_{b0}^i
1	constant 1000 MPa (no rupture)	varied with heating rate
2	constant 1000 MPa (no rupture)	constant (value from 5×10^4 K/s prediction)
3	varied with heating rate	constant (value from 5×10^4 K/s prediction)
4	varied with heating rate	varied with heating rate

Results of this sensitivity analysis are shown in Figure 12. Under the condition that the central bubble did not rupture

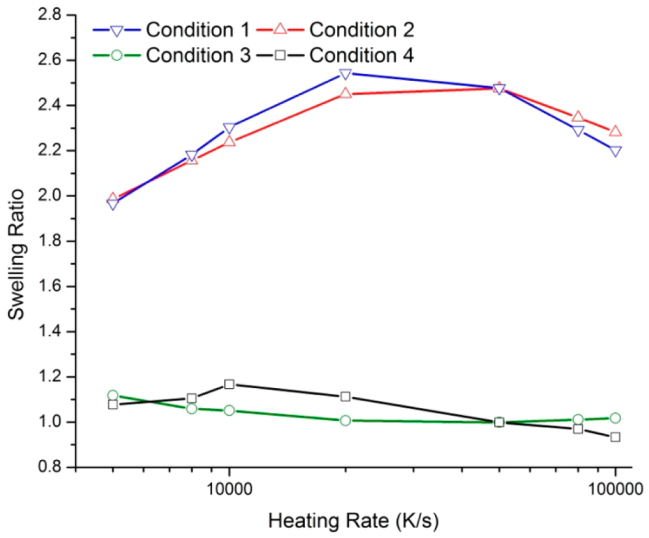

Figure 12. Comparison of simulation results under different computing conditions.

(Condition 1), the final swelling ratio increased and then decreased as the heating rates increased. The increase was due to the increase of the internal pressure; and the deceasing part was due to the decline in duration. Under the computing condition that the initial bubble number in the plastic stage changed with heating rate (Condition 1), the change of the final swelling ratio with heating rate is greater than the condition that the initial bubble number was held constant (Condition 2). It must also be noted that the final swelling ratio is much larger under the condition that the central bubble did not rupture (Condition 1) than the condition that central bubble rupture is considered (Condition 4).

Under the condition that central bubble rupture is considered, if the bubble number was held constant (Condition 3), the increasing then decreasing trend of swelling ratio with increasing heating rates was not observed. In this case, the swelling ratio decreases as the heating rate increases, because of the increasing bubble rupture frequency below the heating rate of 5×10^4 K/s. However, when the heating rate is larger than 5×10^4 K/s, because the duration of the plastic phase is so short at the high heating rate, the swelling ratio increases slightly, because there is not sufficient time for bubble rupture. However, under the computing condition that the initial bubble number in plastic stage changes with heating rates (Condition 4), the increasing (then decreasing) trend of swelling ratio with increasing heating rates is observed. This indicates that, at 0.1 MPa, the changes of initial bubble number in the plastic stage with heating rate is the dominant factor for the increasing (then decreasing) trend of swelling ratio with increasing heating rates.

In addition, because the initial bubble number in the plastic stage is controlled by the initial pressure of plastic stage, the more obvious increasing (then decreasing) trend of swelling ratio with increasing heating rates under the computing condition that the initial bubble number in the plastic stage changed with heating rate also indicates that the influence of the initial pressure of plastic stage on swelling is important.

3.4. Influence of Ambient Pressure. The pyrolysis of the 60-μm coal particles of Illinois No. 6 bituminous coal and Pittsburgh No. 8 bituminous coal at various heating, ambient pressure, and a heating rate of 1×10^4 K/s were simulated. The final swelling ratio increased first and then decreased with increasing ambient pressure, as shown in Figure 13, which

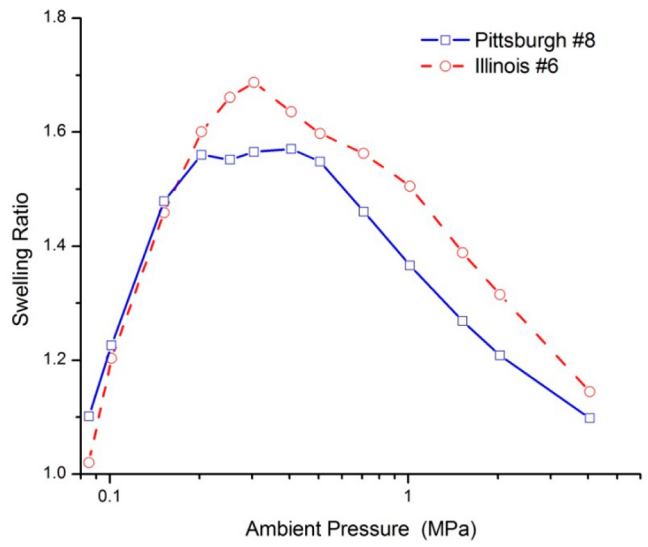

Figure 13. Final swelling ratio at various ambient pressures and a heating rate of 1×10^4 K/s.

agrees with the trend observed in similar experiments.[15] The predicted trend of final swelling ratio with the increase of the ambient pressures at different heating rates and particle sizes is compared with experimental data in Figure 14. The predictions agree with the data for the Pittsburgh No. 8 and the Australian bituminous coals at all pressures. The predicted swelling ratios for the Illinois No. 6 coal match the trend at most pressures. However, the predicted swelling ratio at 0.8 MPa for the Illinois No. 6 coal is much smaller than the reported data. Even if it is assumed that the central bubble does not rupture, at the ambient pressure of 0.1 MPa and the heating rate of 5×10^4 K/s, at which the swelling driving force is bigger and the initial bubble number is larger, the predicted swelling ratio is much smaller than the data (see Figure 12). This may be due to the limitation of the single central bubble assumption in the model. The Illinois No. 6 bituminous coal data were obtained at a

dx.doi.org/10.1021/ef5016846 | Energy Fuels 2014, 28, 7216−7226

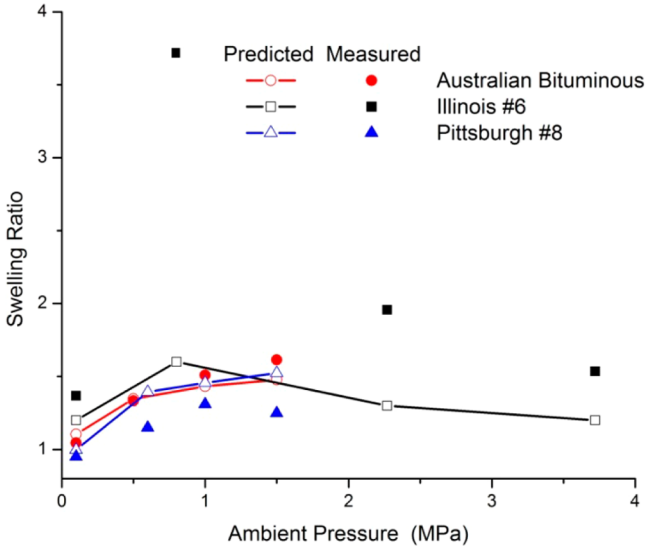

Figure 14. Comparison of the predicted trend of final swelling ratio of coal particle with increasing ambient pressures to experimental data. (Coal particle sizes and heating rates: Pittsburgh No. 8, 75 μm and 1.0 $\times$ 10^5; Illinois No. 6, 62 μm and 1.0 $\times$ 10^4; Australian Bituminous, 63–90 μm and 6.6 $\times$ 10^4.)[6,14,31]

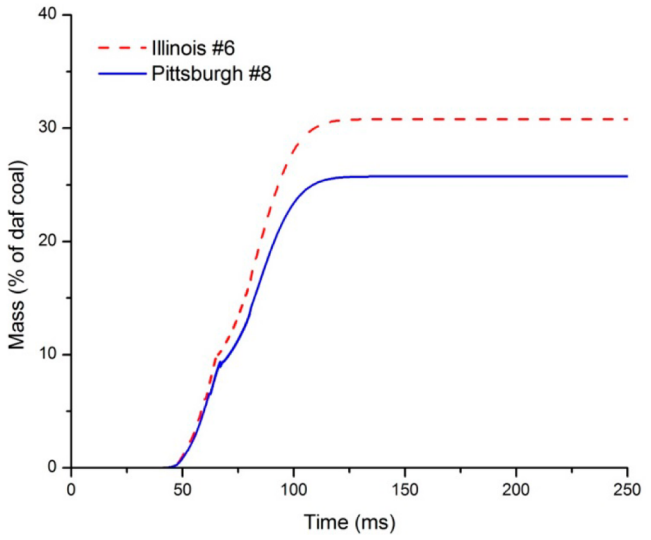

Figure 15. Predicted yields of gases during pyrolysis at a heating rate of 1 $\times$ 10^4 K/s and an ambient pressure of 0.1 MPa.

heating rate of 1 $\times$ 10^4 K/s, which is less than that of the other two coals, whose heating rates were 6.6 $\times$ 10^4 K/s and 1 $\times$ 10^5 K/s. At a lower heating rate and a higher ambient pressure, the pressure difference between inside and outside the particle at the beginning of the plastic stage is smaller. The initial sizes of the surrounding bubbles are larger. Under these conditions, it may be more likely that more than one central bubble is formed in the particle. Finally, swelling prediction may also be limited by in the accuracy of the correlations for temperature-dependent viscosity of the coal particle or other limitations of the model.

The effect of ambient pressure on particle swelling during pyrolysis is complicated, but is explained in the following two points:

(1) Increasing ambient pressure reduces the pressure difference between the inside and outside of the particle. Decreasing the pressure difference reduces the rupture frequency of the large central bubble in the single bubble stage, which increases particle expansion. In Figure 7, at an ambient pressure of 0.1 MPa and all heating rates, the swelling ratios of Illinois No. 6 bituminous coal are smaller than Pittsburgh No. 8 bituminous coal. The main reason for this result is that the light gas yield of Illinois No. 6 bituminous coal is greater than Pittsburgh No. 8 bituminous coal. In the late stage of pyrolysis, the light gas generation rate of Illinois No. 6 coal is much higher (see Figure 15), which makes the internal pressure of Illinois No. 6 coal larger and the central bubble ruptures more easily. At higher ambient pressures, part of the internal pressure can be counteracted and the rupture frequency of the central bubble decreases. The swelling ratio increases with increasing ambient pressure. At higher internal pressures, the rupture frequency of Illinois No. 6 bituminous coal decreases more than Pittsburgh No. 8 bituminous coal, and the gap becomes smaller at high ambient pressures. Therefore, with a close rupture frequency of the central bubble, the larger internal pressure in Illinois No. 6 bituminous makes the particle swell slightly more than in Pittsburgh No. 8 bituminous (see Figure 13).

(2) With a smaller pressure difference, the driving force of swelling decreases. Too high of an ambient pressure restrains the swelling of the bubbles and the swelling ratio decreases.

In addition, the increasing ambient pressure can restrain the vaporization of Metaplast. Increased Metaplast increases the plasticity of the particle and extends the duration of the plastic stage (see Figure 16), which increases plastic deformation. With

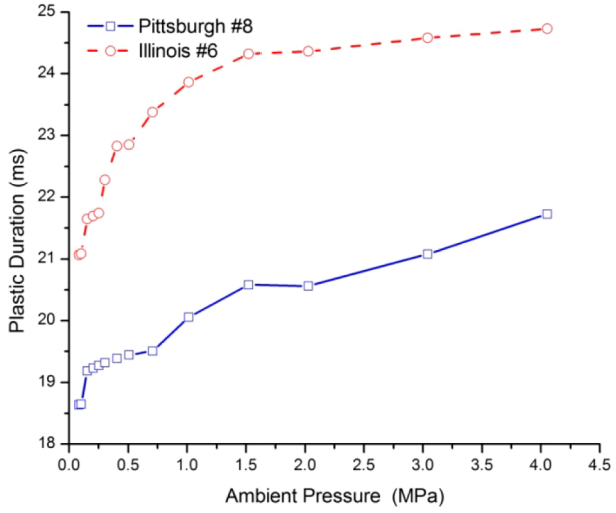

Figure 16. Duration of the plastic stage at various ambient pressures and a heating rate of 1 $\times$ 10^4 K/s.

increasing ambient pressure, both the initial pressure and the initial number of bubbles in the plastic stage decrease, as does particle swelling.

At an elevated ambient pressure, the swelling ratio also increases and then decreases as the heating rates increase. However, the peak of the swelling ratio becomes larger and moves to higher heating rates with the increasing ambient pressure, as shown in Figure 17. The change of the swelling ratio with the increase in heating rate is larger at a larger ambient pressure, which is caused by the smaller rupture frequency, and the increasing pressure difference between the inside of the particle and the outside of the particle and its

dx.doi.org/10.1021/ef5016846 | Energy Fuels 2014, 28, 7216–7226

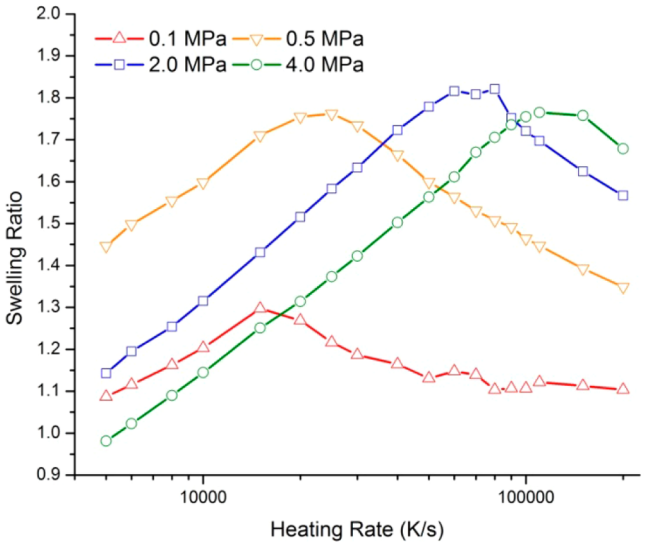

Figure 17. Predicted final swelling ratio at various heating rates and various ambient pressures (60-μm coal particle of Illinois No. 6 bituminous).

decreasing duration become the dominant factor for the increasing (then decreasing) trend of swelling ratio with increasing heating rates at an elevated ambient pressure.

4. CONCLUSIONS

A model was developed to predict the swelling ratio of high volatile bituminous coal during pyrolysis, based on the assumption that the initial structure of bubble distribution in the particle at the beginning of the plastic stage is a central bubble surrounded by many surrounding bubbles. The initial number and size of bubbles in the plastic stage are calculated by the pressure in the particle at the end of the preplastic stage. The rupture of surrounding bubbles at the surface of the particle and the coalescence of surrounding bubbles with the central bubble are both considered.

The pyrolysis processes of eight samples of high-volatile bituminous coals are simulated. The results agree well with experimental results, and the change of the particle size during pyrolysis first increases and then decreases.

The final particle swelling ratio increases and then decreases as the heating rate increases. At atmospheric pressure, swelling behavior is due to the increasing then decreasing initial bubble number in the plastic stage with increasing heating rates. However, at an elevated ambient pressure, swelling ratio is dominated by the increasing pressure difference between the inside of the particle and the outside of the particle and the decreasing duration of the pressure spike with increasing heating rates.

The increasing (then decreasing) trend of the particle's final swelling ratio with increasing ambient pressure is predicted. In the lower pressure range, the increase of ambient pressure reduces the rupture frequency of the bubbles and increases the swelling ratio. However, high ambient pressures are better able to counteract the pressure inside the bubbles and decrease the particle swelling.

AUTHOR INFORMATION

Corresponding Author

*E-mail: lisuf@dlut.edu.cn.

Notes

The authors declare no competing financial interest.

ACKNOWLEDGMENTS

This work is supported in part by a scholarship from the China Scholarship Council (CSC), under the Grant CSC No. 201306060059, and performed at Brigham Young University while H.Y. was a visiting graduate student. Thanks to Andrew Richards, who helped edit the manuscript.

REFERENCES

(1) Fong, W. S.; Peters, W. A.; Howard, J. B. Kinetics of generation and destruction of pyridine extractables in a rapidly pyrolysing bituminous coal. *Fuel* **1986**, *65* (2), 251−254.

(2) Fong, W. S.; Khalil, Y. F.; Peters, W. A.; Howard, J. B. Plastic behaviour of coal under rapid-heating high-temperature conditions. *Fuel* **1986**, *65* (2), 195−201.

(3) Oh, M. S.; Peters, W. A.; Howard, J. B. An Experimental and Modeling Study of Softening Coal Pyrolysis. *AIChE J.* **1989**, *35* (5), 775−792.

(4) Sheng, S.; Azevedo, J. L. T. Modeling the evolution of particle morphology during coal devolatilization. *Proc. Combust. Inst.* **2000**, *28*, 2225−2232.

(5) Bayless, D. J.; Schroeder, A. R.; Peters, J. E.; Buckius, R. O. Effects of surface voids on burning rate measurements of pulverized coal at diffusion-limited conditions. *Combust. Flame* **1997**, *108*, 187−198.

(6) Zeng, D.; Clark, M.; Gunderson, T.; Hecker, W. C.; Fletcher, T. H. Swelling properties and intrinsic reactivities of coal chars produced at elevated pressures and high heating rates. *Proc. Combust. Inst.* **2005**, *30*, 2213−2221.

(7) Bailey, J. G.; Tate, A.; Diessel, C. F. K.; Wall, T. F. A char morphology system with applications to coal combustion. *Fuel* **1990**, *69*, 225−239.

(8) Yu, J.; Lucas, J. A.; Wall, T. F. Formation of the structure of chars during devolatilization of pulverized coal and its thermoproperties: A review. *Prog. Energy Combust. Sci.* **2007**, *33*, 135−170.

(9) Gao, H.; Murata, S.; Nomura, M. Experimental Observation and Image Analysis for Evaluation of Swelling and Fluidity of Single Coal Particles Heated with CO_2 Laser. *Energy Fuels* **1997**, *11*, 730−738.

(10) Yu, J.; Strezov, V.; Lucas, J.; Wall, T. Swelling behaviour of individual coal particles in the single particle reactor. *Fuel* **2003**, *82* (16), 1977−1987.

(11) Zygourakis, K. Effect of pyrolysis conditions on the macropore structure of coal derived chars. *Energy Fuels* **1993**, *7* (1), 33−41.

(12) Gale, T. K.; Bartholomew, C. H.; Fletcher, T. H. Decreases in the swelling and porosity of bituminous coals during devolatilization at high heating rates. *Combust. Flame* **1995**, *100* (1−2), 94−100.

(13) Shurtz, R. C.; Kolste, K. K.; Fletcher, T. H. Coal swelling model for high heating rate pyrolysis applications. *Energy Fuels* **2011**, *25*, 2163−2173.

(14) Lee, C. W.; Scaroni, A. W.; Jenkins, R. G. Effect of pressure on the devolatilization and swelling behavior of a softening coal during rapid heating. *Fuel* **1991**, *70* (8), 957−965.

(15) Shurtz, R. C.; Hogge, J. W.; Fletcher, T. H. Coal swelling model for pressurized high particle heating rate pyrolysis applications. *Energy Fuels* **2012**, *26*, 3162−3627.

(16) Solomon, P. R.; Serio, M. A.; Hamblen, D. G.; Smoot, L. D.; Brewster, B. S.; Radulovic, P. T. *Measurement and Modeling of Advanced Coal Conversion Processes*, Final Report, No. DE96000577; Advanced Fuel Research, Inc.: Morgantown, WV and Brigham Young University: Provo, Utah, 1993; pp 71−73.

(17) Griffin, T. P.; Howard, J. B.; Peters, W. A. An experimental and modeling study of heating rate and particle size effects in bituminous coal pyrolysis. *Energy Fuels* **1993**, *7* (2), 297−305.

(18) Yu, J.; Strezov, V.; Lucas, J.; Liu, G.; Wall, T. A mechanistic study on char structure evolution during coal devolatilization—

Experiments and model predictions. *Proc. Combust. Inst.* **2002**, *29* (1), 467−473.
(19) Yu, J.; Lucas, J.; Wall, T. Modeling the development of char structure during the rapid heating of pulverized coal. *Combust. Flame* **2004**, *136*, 519−532.
(20) Yu, Y.; Xu, M.; Yu, D.; Huang, J. Fragmentation of coal particles by devolatilization during combustion. *J. Huazhong Univ. Sci. Technol.* **2005**, *3*, 78−80.
(21) Wu, Z.; Zhang, C. l.; Chen, H. Establishment of Fragment Model of Coal during Combustion. *J. Fuel Chem. Technol.* **2003**, *31* (1), 17−21.
(22) Yang, H.; Li, S.; Fletcher, T. H.; Dong, M.; Zhou, W. Simulation of the Evolution of Pressure in a Lignite Particle during Pyrolysis. *Energy Fuels* **2014**, *28*, 3511−3518.
(23) Grant, D. M.; Pugmire, R. J.; Fletcher, T. H.; Kerstein, A. R. Chemical model of coal devolatilization using percolation lattice statistics. *Energy Fuels* **1989**, *3*, 175−186.
(24) Fletcher, T. H.; Kerstein, A. R.; Pugmire, R. J.; Grant, D. M. Chemical percolation model for devolatilization. 2. Temperature and heating rate effects on product yields. *Energy Fuels* **1990**, *4*, 54−60.
(25) Fletcher, T. H.; Kerstein, A. R.; Pugmire, R. J.; Solum, M. S.; Grant, D. M. Chemical percolation model for devolatilization. 3. Direct Use of ^{13}C NMR Data to Predict Effects of Coal Type. *Energy Fuels* **1992**, *6* (4), 414−431.
(26) Fletcher, T. H.; Hardesty, D. R. *Compilation of Sandia Coal Devolatilization Data*: Milestone Report, No. SAND92-8209; Sandia National Laboratories: Livermore, CA, USA, 1992; pp 5−43.
(27) Ma, L. *Combustion and gasification of chars in oxygen and carbon dioxide at elevated pressure*. Ph.D. Thesis, Stanford University, Stanford, CA, 2006.
(28) Attar, A. Bubble nucleation in viscous material due to gas formation by a chemical reaction: Application to coal pyrolysis. *AIChE J.* **1978**, *24* (1), 106−115.
(29) Gan, H.; Nandi, S. P.; Walker, P. L. Nature of the porosity in American coals. *Fuel* **1972**, *51*, 272−277.
(30) Serio, M. A.; Hamblen, D. G.; Markham, J. R.; Solomon, P. R. Kinetics of volatile product evolution in coal pyrolysis: experiment and theory. *Energy Fuels* **1987**, *1* (2), 138−152.
(31) Wu, H.; Bryant, G.; Benfell, K.; Wall, T. An Experimental Study on the Effect of System Pressure on Char Structure of an Australian Bituminous Coal. *Energy Fuels* **2000**, *14* (2), 282−290.